Water SA 46(3) 500–505 / Jul 2020
https://doi.org/10.17159/wsa/2020.v46.i3.8660

Photocatalytic degradation of a basic dye in water by nanostructured HPEI/TiO_2 containing membranes

Penny Mathumba[1], Khona Maziya[1], Alex T Kuvarega[2], Langelihle N Dlamini[1] and Soraya P Malinga[1]

[1]Department of Chemical Sciences, University of Johannesburg, P.O. Box 17011, Doornfontein, Johannesburg 2028, South Africa
[2]Nanotechnology and Water Sustainability Research Unit (NanoWS), College of Science, Engineering and Technology (CSET), University of South Africa (UNISA), Florida Science Campus, South Africa

A photocatalytically active membrane was synthesized through the embedding of HPEI/TiO_2 nanocomposite in PES membrane for the removal of methyl orange (MO) dye from water. Membranes were characterized using scanning electron microscopy coupled with energy dispersive X-ray, atomic force microscopy, water contact angle measurements and water flux analysis. PES/HPEI/TiO_2 membranes showed improved hydrophilicity and were effective in the photodegradation of MO. The reaction rate for MO degradation was 11.6 x 10^{-3} min^{-1}, and the degradation was accompanied by the generation of sulphate ions as degradation by-products.

CORRESPONDENCE
Soraya P Malinga

EMAIL
smalinga@uj.ac.za

DATES
Received: 20 June 2019
Accepted: 2 June 2020

KEYWORDS
hyperbranched polymers
methyl orange
phase inversion
polyethersulfone membranes
titanium dioxide nanoparticle

INTRODUCTION

The use of a photocatalytically active membrane has received attention of late in the degradation of dyes (e.g. methyl orange, MO) in water. A multi-functional system that incorporates the attractive qualities of both membrane filtration and photocatalysis will synergistically achieve physical separation by membrane filtration and organic degradation in a single unit (Xu et al., 2018; Li et al., 2019). The utilisation of photocatalytic membranes promotes photocatalyst separation from treated water and thus enhances this application (Bellardita et al., 2020).

Titanium dioxide (TiO_2) is mostly used because of its high stability, low cost, non-toxicity, high turnover number, flexibility, strong oxidizing power, stability against photocorrosion and chemical resistance (Anwer et al., 2019; Dhanasekar et al., 2018). TiO_2 based photocatalysts possess a large surface area, which can signify high photocatalytic efficiency (Hoseini et al., 2017). The TiO_2 band gap is approximately 3.2 eV and its photocatalytic activity is restricted to the ultraviolet region since it cannot absorb visible light (Han et al., 2017). There are different crystal structures of TiO_2, anatase, brookite and rutile. The anatase phase has gained more recognition owing to its increased photoactivity (Leong et al., 2014). To achieve its maximum efficiency, TiO_2 nanoparticles have previously been immobilised on polymer films (Yan et al., 2017; Kuvarega et al., 2018; Pereira et al., 2015).

In this study, polyethersulfone (PES) and hyperbranched polyethyleneimine (HPEI) were used as immobilizers for anatase TiO_2 to form a photocatalytically active membrane. HPEI was used as a template and dispersing agent for the synthesis of TiO_2 nanoparticles. HPEI has cavities that act as hosts for nanoparticle synthesis through electrostatic attractions between the nitrogen groups, thus producing uniform and well-dispersed nanoparticles (Koloti et al., 2018; Mathumba et al., 2017). In our previous study HPEI played a significant role in the production of small and well-dispersed TiO_2 nanoparticles (Mathumba et al., 2017). Moreover, these nanocavities accommodate the catalyst and act as adsorption sites for degradation and removal of organic pollutants. Moreover, the amine groups on the peripheral region of HPEI induce hydrophilicity on the membrane (Vlotman et al., 2018; Mosikatsi et al., 2019).

Introduction of PES in the system induces membrane properties such as hydrothermal, mechanical and chemical stability (Safarpour et al., 2016; Rajabi et al., 2015; Nasrollahi et al., 2019). The use of HPEI/TiO_2 nanocomposite embedded in PES for the removal of MO in water has not previously been reported. Thus, this study is aimed at fabricating and applying PES/HPEI/TiO_2 for the photocatalytic degradation of MO dye under ultraviolet (UV) light.

EXPERIMENTAL

Materials

HPEI (Lupasol WF, Mw:25 kDa) was supplied by Caltech (California, USA) and used as received. Solvay provided PES (Mw 3000 P, India). Other chemicals and reagents used in this study were used as received.

Fabrication of PES/HPEI/TIO_2 photocatalytic membrane

TiO_2 nanoparticles were prepared according to a previously reported method by Mathumba et al. (2017). To prepare the HPEI/TiO_2 composite, HPEI (9.83 mmol) was first dissolved in deionised water (5 mL). From this solution, varying concentrations of HPEI:TiO_2 were prepared by adding TiO_2 nanoparticles

to the HPEI solution. The solutions were stirred for 2 h and consequently sonicated for another 2 h. The resulting slurry was then heated for 5 h at 60°C to remove the solvent and then dried in an oven for 2 h at 90°C to remove excess moisture.

Flat sheet membranes were prepared by using the phase inversion method. PES powder (16 wt%) was dissolved in NMP and stirred for 2 h. HPEI/TiO_2 nanocomposite (0.05%, 0.10%, 0.50% and 1.00 wt%) was added into the PES dope solution under continuous stirring to attain varying concentrations of PES nanocomposite polymer. The solution was stirred overnight at a temperature of 80°C and further degassed using nitrogen gas to remove air bubbles formed during the reaction. A casting knife set at an air gap of 200 µm was used to cast the membranes on a glass plate. The casting solution was poured on the edge of the glass plate and spread on the glass plate using the casting knife. The glass plate was immediately placed into a non-solvent coagulation bath containing deionised water at 4°C for 30 min. The resulting membranes were dried at room temperature and stored in between sheets of paper.

Characterization of membranes

Morphological assessment

To assess the surface and cross-section (CS) of the membranes, SEM (TESCAN Vega TC instrument, VEGA 3TESCAN software) was utilised. For CS image analysis, the membrane samples were frozen in liquid nitrogen, fractured and coated with gold. Scanning electron microscopy (SEM) images were analysed at an accelerating voltage of 2 kV using a TESCAN Vega TC instrument (VEGA 3TESCAN software), equipped with X-ray detector for energy dispersive X-ray analysis (EDX) operated at 5 kV. The surface morphology and the roughness (Rq) of the membranes were measured using a Veeco Dimension 3100 atomic force microscopy (AFM) equipped with Nanoscope V530 r3sr3 software. Prior to analysis, the samples were mounted on a carbon tape and coated with carbon for enhanced images.

Water contact angle

Surface wetting properties of the membranes as a function of the concentration of TiO_2 nanoparticles were evaluated through water contact angle measurements. Contact angle measurements were conducted using the sessile drop method on a Data Physics Optical instrument (SCA20 software) using water as a probe. An average of 10 measurements was conducted per sample at room temperature.

Water intake capacity (WIC) measurements

The extent of water absorption by membranes was determined through sorption experiments. Membrane samples (25 cm^2) were soaked in distilled water for 24 h, and thereafter mopped with blotting paper and weighed to give the wet weight ($^w w$). The membranes were then dried at 60°C for 24 h in an oven to obtain the dry weight ($^w d$) of the membranes. The analyses were performed in replicate.

The water intake capacity was calculated using Eq. 1.

$$\text{Water intake capacity (\%)} = \frac{w_w - w_d}{w_w} \times 100\% \quad (1)$$

where: w_w and w_d are the weights of wet and dry membranes, respectively.

Membrane flux studies

Membrane flux studies were conducted on a Sterlitech corporation CF042SS316 S/NJC164 207613 cross flow instrument. The membranes were compacted for 12 h at 250 Pa for stabilization of flux before analysis. Four different pressures were used for the pure water flux studies, namely, 50, 100, 150 and 200 Pa. The analyses were performed in replicate. The flux was calculated using Eq. 2:

$$J_w = \frac{V}{T \times A} \quad (2)$$

where: J_W ($L{\cdot}m^{-2}{\cdot}h^{-1}$) is the pure water flux, V is the volume of the permeate (m^3), T is the permeation time (h) and A is the effective membrane surface (36 cm^2).

Photocatalytic degradation of methyl orange using PES/HPEI/TiO_2 membranes and degradation by-products

Photocatalytic tests were performed using batch experiments. Photocatalytic degradation of MO dye was conducted by cutting small pieces of membranes (25 cm^2). The membranes were individually immersed into 500 mL beakers covered with parafilm, containing MO dye (10 mg/L, 250 mL) solutions and equilibrated for 1 h in the dark while stirring. The UV light source for the excitation of TiO_2 was set at a wavelength of 365 nm. Aliquots (5 mL) of the samples were collected at 10 min interval for a maximum period of 2 h using a syringe. The photocatalytic studies were conducted at different pH values (2, 5, 7, 9 and 12) and these were adjusted using 0.1 M NaOH and 0.1 M HCl. The degradation of MO dye was monitored by measuring the absorbance at λ = 464 nm, as a function of irradiation time, using a UV-Vis spectrophotometer (Shimadzu UV-2450). All measurements were done in replicate. The photocatalytic degradation was calculated using Eq. 3:

$$\text{\% removal} = (1 - \frac{c_t}{c_0}) \times 100\% \quad (3)$$

where: C_0 and C_t are the initial and final concentrations of the dyes at t = 0 minutes and t = t min, respectively. The resulting degradation by-products of MO, i.e., SO_4^{2-} ions, were analysed using ion chromatography (IC-Dionex-IC2000). The eluent solution was 30.00 mM KOH. The pump pressure was set at 1630 psi, column heater at 30°C and run time was 11 min/sample.

RESULTS AND DISCUSSION

SEM analysis

Figure 1 represents the surface, CS and AFM images of the membranes. The pristine PES exhibited a highly porous surface, uniform finger-like structure with a thin skin layer and large ridges (Fig. 1 A, A', A"). Upon addition of HPEI/TiO_2 the pores became reduced due to the accumulation of the HPEI/TiO_2 nanocomposite (Fig. 1 A–E). The CS images (Fig. 1 A'–E') show a sponge-like structure with a dense skin layer for the blended membranes as opposed to the pure PES membrane. As the composition of HPEI/TiO_2 was increased in the membranes, the macrovoids in the sponge-like membrane became more pronounced (Fig. 1 B'–E'). The addition of HPEI/TiO_2 composite changes the kinetics and the thermodynamics of the phase inversion process by reducing the hydraulic resistance due to its hydrophilicity. The increased affinity of the HPEI/TiO_2 nanocomposite resulted in a faster exchange between the solvent and non-solvent during phase inversion thus leading to the formation of a sponge-like structure with macrovoids (Xu et al., 2017; Ayyaru and Ahn, 2018).

It was observed from the AFM images (Fig. 1 A"–E") that the surface properties of the PES membranes improved due to blending with HPEI/TiO_2. As the concentration of HPEI/TiO_2 increased, the ridges decreased in size, indicating a decrease in surface roughness of the blend membranes. The roughness measurements illustrated in Table 1 showed a decrease from 40 nm (pristine PES) to 18.9 nm for the modified membranes. The migration and accumulation of HPEI/TiO_2 nanocomposites on the surface pores leads to the reduction of surface pores and roughness (Liu et al., 2007). A similar trend was observed by Parvizian et al. (2020), where TiO_2 was functionalized with oleic acid and embedded on a PES membranes via phase inversion. AFM measurements decreased from 24 nm (unmodified membrane) to 4 nm (modified membrane).

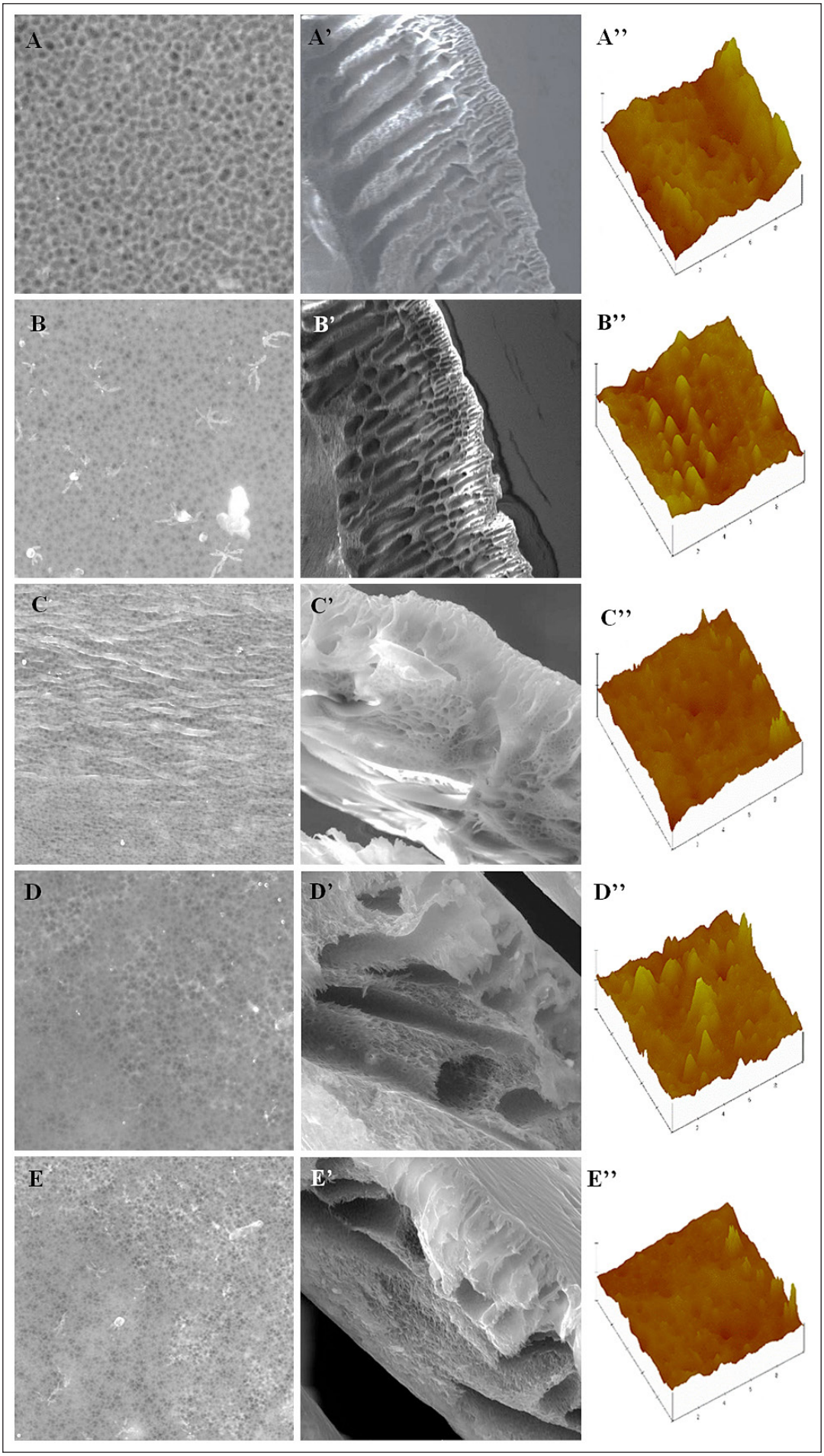

Figure 1. SEM surface, CS and AFM images of PES (A, A′ and A″) 0.05% HPEI/TiO2 (B, B′ and B′), 0.10% HPEI/TiO2 (C, C′ and C″), 0.50% HPEI/TiO2 (D, D′ and D″) and 1.00% HPEI/TiO2 membranes (E, E′ and E″)

Table 1. Contact angle, water intake capacity and membrane roughness studies

PES/HPEI/TiO_2 membrane (%)	Contact angle (°)	Water intake capacity (%)	Membrane roughness (nm)
0.00	76.5	8.32	40.3
0.05	69.0	26.67	37.5
0.10	65.3	38.82	28.0
0.50	62.8	41.86	34.3
1.00	66.2	35.28	18.9

This was attributed to the nanoparticles that migrate to fill in the pores and the free volume in the surface of the membranes due to the migration of OA-TiO_2 to the membrane surface.

Water permeation studies of PES/HPEI/TiO_2 membranes

The contact angle measurements were performed to evaluate the hydrophilicity of the membrane. Generally, the contact angle of PES/HPEI/TiO_2 membranes decreased as the HPEI/TiO_2 loadings were increased from 0.05% to 0.10% (Table 1). The presence of hydrophilic TiO_2 and HPEI enhanced hydrophilicity of the membranes, due to the NH_2 and –OH groups from HPEI and TiO_2, respectively (Xu et al., 2018; Wang et al., 2017). This increase in contact angle at high HPEI/TiO_2 content may be attributed to the migration of hydrophobic cavities of the HPEI polymer to the surface of the membrane during the drying process (Safarpour et al., 2016). The WIC for modified membranes increased with increasing nanocomposite loading (Table 1). The WIC values for the neat PES membrane were low, due to its hydrophobic nature.

Water flux analysis

The pure water flux was measured at different applied pressures and the results showed a good linear relationship between the two parameters ($R^2 \approx 0.98$). The flux increased with an increase in operating pressure. The PES membrane showed higher water flux as compared to PES/HPEI/TiO_2 membranes (Fig. 2). The low water permeability of the modified membranes could be due to the HPEI/TiO_2 nanocomposites blocking the surface pores of the membranes. This creates a dense membrane surface layer, thus resulting in high resistance to water passing through the membrane resulting in reduced permeability. Tavakolmoghadam and Mohammadi (2019) observed a decrease in water flux with the increase of TiO_2 in PVDF membrane. This was due to the agglomeration of TiO_2 nanoparticles thus blocking the surface pores of the membranes.

Photocatalytic activity of PES/HPEI/TiO_2 membranes

The PES/HPEI/TiO_2 membranes were evaluated for their ability to degrade MO at different pH conditions under UV light radiation. It was observed that the neat PES membrane exhibited low dye removal (less than 5% in acidic, neutral and alkaline conditions) since the polymer is not photocatalytically active.

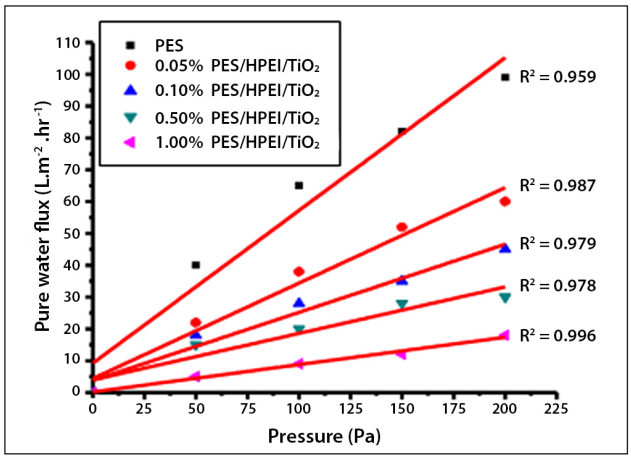

Figure 2. A plot of pressure versus pure water flux

Faster degradation rates were observed in the first 5 min of the reactions for all modified membranes. The rate then decreased with time up to 80 min due to the saturation of membrane reactive sites. However, all the membranes showed optimal activity at pH 2 for degradation of MO dye. For comparison, the kinetics of MO degradation at pH 2 were evaluated for all the membrane samples (Fig. 3A). It was observed that the PES membrane shows 4.26% removal of 10 mg/L MO. However, the percentage removal of MO increased upon introduction of HPEI/TiO_2 nanocomposites on the PES membranes, which then reached the highest removal of 70.3% at 0.50% HPEI/TiO_2 loading and a decline to 59.2% at 1.00% HPEI/TiO_2 loading. This is an indication that nanocomposite percentage loadings above 0.50% on the membranes result in membrane saturation and, therefore, are not effective for the degradation of dyes. It can be observed from Fig. 3B that the photodegradation of MO under UV light radiation follows pseudo-first order reactions and the kinetics can be described by the general Eq. 4:

$$-In\frac{C}{C_0} = kt \quad (4)$$

where k is the reaction constant, C_0 and C are the initial and final concentrations of MO and t is time respectively. Among these photocatalytically active membranes, the 0.50% PES/HPEI/TiO_2 membrane showed the highest reaction rate (11.6 x 10^{-3} min^{-1}) when illuminated with UV light, thus exhibiting the highest percentage removal of MO as compared to the other membranes.

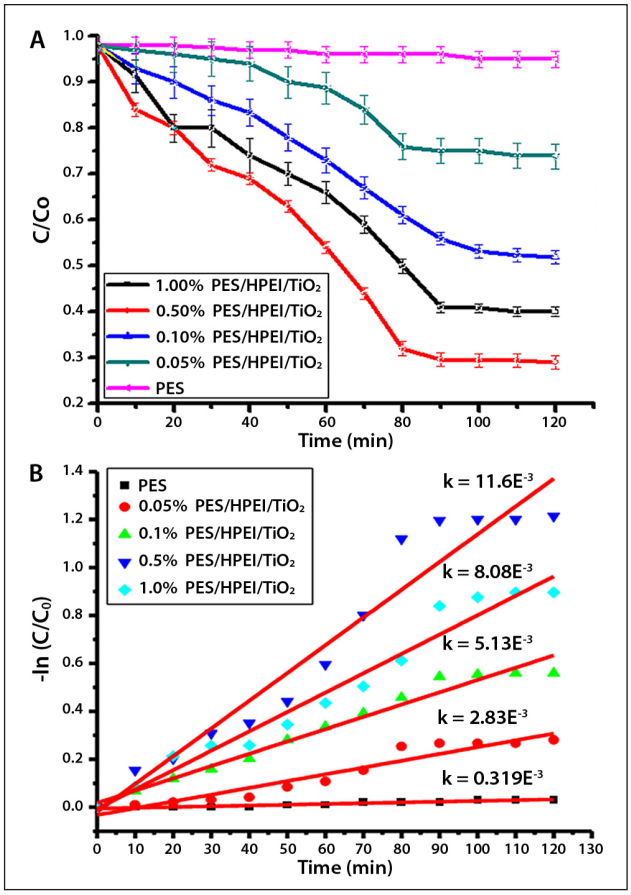

Figure 3. Degradation of MO by PES/HPEI/TiO_2 membranes at pH 2 (A); Reaction kinetics of MO dye degradation initiated by UV light irradiation (B)

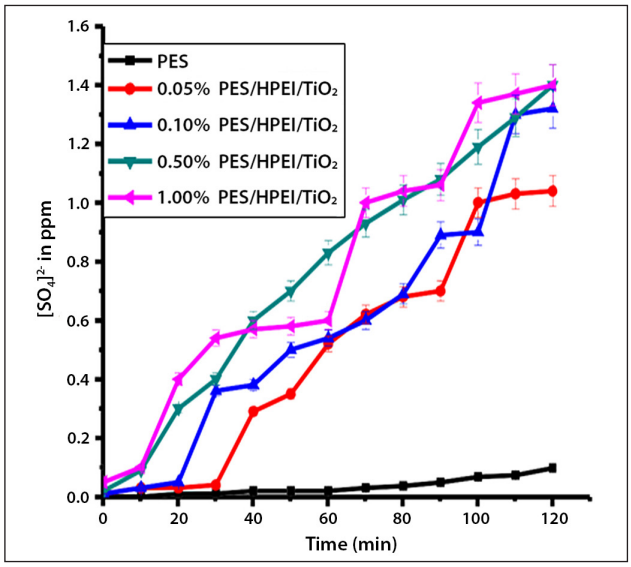

Figure 4. Generation of sulphate ions from the degradation of MO using PES/HPEI/TiO_2 photocatalytic membranes at pH 2

Photodegradation by-products

Figure 4 illustrates the generation of degradation by-product of MO dye (SO_4^{2-}) as a function of time. The degradation of MO was confirmed by the liberation of SO_4^{2-} ions using IC. The sulphite ion can be oxidized to sulphate, a more stable (+6) oxidation state of sulphur, and hence it was more reasonable to measure than the sulphite ion. Studies reveal that sulphates adsorb irreversibly on TiO_2 surfaces, and this might have accounted for the low amounts of sulphate ions detected (Liao et al, 2013; Sonawane et al, 2004; Han and Bai, 2010).

CONCLUSION

Photocatalytically active PES/HPEI/TiO_2 membranes were synthesized using varying concentrations of HPEI/TiO_2 nanocomposite. The PES/HPEI/TiO_2 membranes showed improved hydrophilicity, water intake capacity and ability to degrade MO dye in water under UV radiation as compared to pristine PES membrane. The PES/HPEI/TiO_2 (0.50%) membrane exhibited the highest dye removal ability. Thus, these membranes could be applicable in the photocatalytic degradation of organic compounds in highly acidic, neutral and alkaline wastewater.

ACKNOWLEDGEMENTS

The authors would like to thank the Water Research Commission (Project No. K5/2488/3), the Thuthuka National Research Foundation (TTK180427324698), DST/Mintek Nanotechnology Innovation Centre-Water Research Node, National Nanoscience Postgraduate Teaching and Training Programme (NNPTTP), Centre for Nanomaterials Research (University of Johannesburg) and the University of Johannesburg (Faculty of Science) for funding.

DISCLOSURE STATEMENT

No potential conflict of interest was reported by authors.

REFERENCES

ANWER H, MAHMOOD A, LEE J, KIM K, PARK J and YIP A (2019) Photocatalysts for degradation of dyes in industrial effluents: Opportunities and challenges. *Nano Res.* **12** 1–18. https://doi.org/10.1007/s12274-019-2287-0

AYYARU S and AHN Y (2018) Fabrication and separation performance of polyethersulfone/sulfonated TiO_2 (PES–STiO$_2$) ultra filtration membranes for fouling mitigation. *J. Ind. Eng. Chem.* **6** 199–209. https://doi.org/10.1016/j.jiec.2018.06.030

BELLARDITA M, CAMERA-RODA G, LODDO V, PARRINO F and PALMISANO L (2020) REVIEW: Coupling of membrane and photocatalytic technologies for selective formation of high added value chemicals. *Catal. Today* **340** 128–144. https://doi.org/10.1016/j.cattod.2018.09.024

DHANASEKAR M, JENEFER V, NAMBIAR RB, BABU SG, SELVAM SP, NEPPOLIAN B and BHAT SV (2018) Ambient light antimicrobial activity of reduced graphene oxide supported metal doped TiO_2 nanoparticles and their PVA based polymer nanocomposite films. *Mater. Res. Bull.* **97** 238–243. http://doi.org/10.1016/j.materresbull.2017.08.056

HAN F, MAO X and XU Q (2017) Flower-like Au/Ag/TiO_2 nanocomposites with enhanced photocatalytic efficiency under visible light irradiation. *Sci. China Chem.* **60** (4) 521–527. https://doi.org/10.1007/s11426-016-9027-6

HAN H and BAI R (2010) Highly effective buoyant photocatalyst prepared with a novel layered-TiO_2 configuration on polypropylene fabric and the degradation performance for methyl orange dye under UV-Vis and Vis lights. *Sep. Purif. Technol.* **73** 142–150. http://doi.org/10.1016/j.seppur.2010.03.017

HOSEINI SN, PIRZAMAN AK, AROON MA and PIRBAZARI AE (2017) Photocatalytic degradation of 2,4-dichlorophenol by Co-doped TiO_2(Co/TiO_2) nanoparticles and Co/TiO_2 containing mixed matrix membranes. *J. Water Process Eng.* **17** 124–134. http://doi.org/10.1016/j.jwpe.2017.02.015

KOLOTI LE, GULE NP, AROTIBA OA and MALINGA SP (2018) Laccase-immobilized dendritic nanofibrous membranes as a novel approach towards the removal of bisphenol A. *Environ. Technol.* **39** 392–404. https://doi.org/10.1080/09593330.2017.1301570

KUVAREGA AT, KHUMALO N, DLAMINI D and MAMBA BB (2018) Polysulfone/N, Pd co-doped TiO_2 composite membranes for photocatalytic dye degradation. *Sep. Purif. Technol.* **191** 122–133. http://doi.org/10.1016/j.seppur.2017.07.064

LEONG S, RAZMJOU A, WANG K, HAPGOOD K, ZHANG X and WANG H (2014) TiO_2 based photocatalytic membranes: a review. *J. Membr. Sci.* **472** 167–184. http://doi.org/10.1016/j.memsci.2014.08.016

LI Q, JIA R, SHAO J and HE Y (2019) Photocatalytic degradation of amoxicillin via TiO_2 nanoparticle coupling with a novel submerged porous ceramic membrane reactor. *J. Clean. Prod.* **209** 755–761. https://doi.org/10.1016/j.jclepro.2018.10.183

LIAO Y, BRAME J, QUE W, XIU Z, XIE H, LI Q, FABIAN M and ALVAREZ PJ (2013) Photocatalytic generation of multiple ROS types using low-temperature crystallized anodic TiO_2 nanotube arrays. *J. Hazardous Mater.* **260** 434–441. http://doi.org/10.1016/j.jhazmat.2013.05.047

LIU CH, WU JS, CHIU HC, SUEN S and CHU KH (2007) Removal of anionic reactive dyes from water using anion exchange membranes as adsorbers. *Water Res.* **41** 1491–1500. http://doi.org/10.1016/j.watres.2007.01.023

MATHUMBA P, KUVAREGA AT, DLAMINI LN and MALINGA SP (2017) Synthesis and characterisation of titanium dioxide nanoparticles prepared within hyperbranched polyethylenimine polymer template using a modified sol–gel method. *Mater. Lett.* **195** 172–177. http://doi.org/10.1016/j.matlet.2017.02.108

MOSIKATSI BE, MABUBA N and MALINGA SP (2019) Thin film composite membranes consisting of hyperbranched polyethylenimine (HPEI)-cysteamine layer for cadmium removal in water. *Journal of Water Process Eng.* **30** 100686–100696. http://doi.org/10.1016/j.jwpe.2018.10.004

NASROLLAHI N, ABER S, VATANPOUR V and MAHMOODI NM (2019) Development of hydrophilic microporous PES ultrafiltration membrane containing CuO nanoparticles with improved antifouling and separation performance. *Mater. Chem. Phys.* **222** 338–350. https://doi.org/10.1016/j.matchemphys.2018.10.032

PARVIZIAN F, ANSARI F and BANDEHALI S (2020) Oleic acid-functionalized TiO_2 nanoparticles for fabrication of PES-based nanofiltration membranes. *Chem. Eng. Res. Design* **156** 433–441. https://doi.org/10.1016/j.cherd.2020.02.019

PEREIRA VR, ISLOOR AM, BHAT UK, ISMAIL AF, OBAID A and FUN H (2015) Preparation and performance studies of polysulfone-sulfated nano-titania (S-TiO_2) nanofiltration membranes for dye removal. *RSC Adv.* **5** 53874–53885. http://doi.org/10.1039/c5ra07994b

RAJABI H, GHAEMI N, MADAENI SS, DARAEI P, ASTINCHAP B, ZINADINI S and RAZAVIZADEH SH (2015) Nano-ZnO embedded mixed matrix polyethersulfone (PES) membrane : Influence of nanofiller shape on characterization and fouling resistance. *Appl. Surf. Sci.* **349** 66–77. http://doi.org/10.1016/j.apsusc.2015.04.214

SAFARPOUR M, VATANPOUR V and KHATAEE A (2016) Preparation and characterization of graphene oxide/TiO_2 blended PES nanofiltration membrane with improved antifouling and separation performance. *Desalination* **393** 65–78. http://doi.org/10.1016/j.desal.2015.07.003

SONAWANE RS, KALE BB and DONGARE MK (2004) Preparation and photo-catalytic activity of Fe-TiO_2 thin films prepared by sol-gel dip coating. *Mater. Chem. Phys.* **85** 52–57. http://doi.org/10.1016/j.matchemphys.2003.12.007

TAVAKOLMOGHADAM M and MOHAMMADI T (2019) Application of colloidal precipitation method using sodium polymethacrylate as dispersant for TiO_2/PVDF membrane preparation and its antifouling properties. *Polym. Eng. Sci.* **59** (S1) E422–E434. https://doi.org/10.1002/pen.25009

VLOTMAN DE, NGILA JC, NDLOVU T AND MALINGA SP (2018) Hyperbranched polymer integrated membrane for the removal of arsenic (III) in water. *J. Membr. Sci. Res.* **4** (2) 53–62. http://doi.org/10.22079/JMSR.2017.67560.1148

WANG X, WANG Z, WANG Z, CAO Y and MENG J (2017) Tethering of hyperbranched polyols using PEI as a building block to synthesize antifouling PVDF membranes. *Appl. Surf. Sci.* **419** 546–556. http://doi.org/10.1016/j.apsusc.2017.05.037

XU H, DING M, CHEN W, LI Y and WANG K (2018) Nitrogen–doped GO/TiO_2 nanocomposite ultrafiltration membranes for improved photocatalytic performance. *Sep. Purif. Technol.* **195** 70–82. https://doi.org/10.1016/j.seppur.2017.12.003

XU H, DING M, LIU S, LI Y, SHEN Z and WANG K (2017) Preparation and characterization of novel polysulphone hybrid ultrafiltration membranes blended with N-doped GO/TiO_2 nanocomposites. *Polymer* **117** 198–207. http://doi.org/10.1016/j.polymer.2017.04.022

YAN W, CHEN Q, MENG X and WANG B (2017) Multicycle photocatalytic reduction of Cr (VI) over transparent PVA/TiO_2 nanocomposite films under visible light. *Sci. China Mater.* **60** 449–460. https://doi.org/10.1007/s40843-017-9024-9